European Journal of Cardio-Thoracic Surgery 0 (2020) 1–7
doi:10.1093/ejcts/ezz381

ORIGINAL ARTICLE

Cite this article as: Houben IB, Nama N, Moll FL, van Herwaarden JA, Nordsletten DA, Williams DM *et al*. Mapping pre-dissection aortic wall abnormalities: a multiparametric assessment. Eur J Cardiothorac Surg 2020; doi:10.1093/ejcts/ezz381.

Mapping pre-dissection aortic wall abnormalities: a multiparametric assessment

Ignas B. Houben [a,†], Nitesh Nama [b,†], Frans L. Moll[c], Joost A. van Herwaarden[c], David A. Nordsletten[a,d], David M. Williams[e], Himanshu J. Patel[a], C. Alberto Figueroa [b,d] and Nicholas S. Burris [e,*]

[a] Department of Cardiac Surgery, University of Michigan, Ann Arbor, MI, USA
[b] Department of Surgery, University of Michigan, Ann Arbor, MI, USA
[c] Department of Vascular Surgery, University Medical Center Utrecht, Utrecht, Netherlands
[d] Department of Biomedical Engineering, University of Michigan, Ann Arbor, MI, USA
[e] Department of Radiology, University of Michigan, Ann Arbor, MI, USA

* Corresponding author. Department of Radiology, University of Michigan, 1500 E. Medical Center Drive, Cardiovascular Center 5588, SPC-5030, Ann Arbor, MI 48109-5030, USA. Tel: +1-734-768-7169; e-mail: nburris@med.umich.edu (N.S. Burris).

Received 5 October 2019; received in revised form 17 December 2019; accepted 22 December 2019

Key question

Is there a spatial correlation between focal aortic growth, transmural wall stress and the location of intimal tearing?

Key finding(s)

Focal aortic growth and peak cyclic transmural wall stress co-localized with intimal tear location in all cases.

Take-home message

Non-invasive assessment of aortic wall stress and localized growth may help better understand and predict dissection in genetic aortopathy.

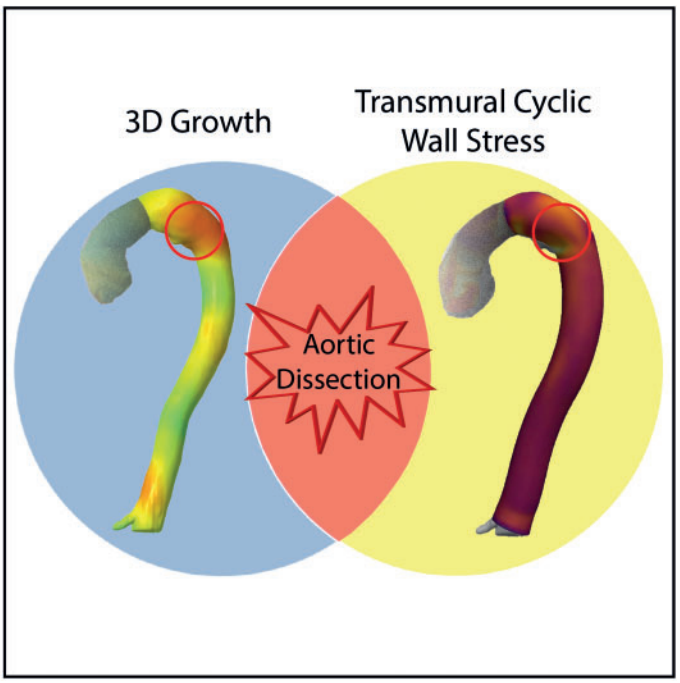

Abstract

OBJECTIVES: Maximal aortic diameter is commonly used to assess aortic risk but poorly predicts the timing and location of dissection events in patients with connective tissue disease who undergo regular imaging surveillance. Hence, we aimed to use available surveillance computed tomography angiography (CTA) scans to investigate the correlation between 3-dimensional (3D) growth and cyclic transmural wall stress with the location of intimal tear formation.

Presented at the 33rd Annual Meeting of the European Association for Cardio-Thoracic Surgery, Lisbon, Portugal, 3–5 October 2019.
†The first two authors contributed equally to this study.

METHODS: Three type B aortic dissection patients with 2 available electrocardiogram (ECG)-gated pre-dissection CTA scans and without surgical repair during the pre-dissection interval were retrospectively identified at our institution. Vascular deformation mapping was used to measure 3D aortic growth between 2 pre-dissection clinical CTA studies. In addition, we performed a computational analysis to estimate cyclic transmural wall stress in patient-specific baseline CTA geometries.

RESULTS: In all 3 connective tissue disease patients, the site of type B aortic intimal tear co-localized with areas of peak 3D aortic wall growth. Aortic growth was detected by clinical radiological assessment in only 1 case. Co-localization of peak transmural stress and the site of intimal tear formation were found in all cases.

CONCLUSIONS: Focal areas of growth and transmural wall stress co-localized with the site of intimal tear formation. These hypothesis-generating results suggest a possible new analytic pathway for a more sophisticated assessment of the factors leading to the initiation of dissection in patients with connective tissue disease. These methods could improve on current risk-stratification techniques.

Keywords: Type B aortic dissection • Aortic growth • Transmural wall stress • Diameter measurement • Vascular deformation mapping

ABBREVIATIONS

CTA	Computed tomography angiography
CTD	Connective tissue disease
TBAD	Type B aortic dissection
VDM	Vascular deformation mapping
3D	3-Dimensional

INTRODUCTION

Type B aortic dissection (TBAD) is a life-threatening condition that requires acute medical attention with antihypertensive treatment and potential surgical intervention [1, 2]. Despite significant advances in surgical techniques for the treatment of TBAD, the ability to predict the timing and location of dissection formation is lacking. A variety of clinical risk factors for TBAD are known, such as advanced age, hypertension, atherosclerosis and connective tissue disease (CTD) [3, 4]. Specifically, patients with CTD (e.g. Marfan syndrome) have a high lifetime risk of dissection and undergo regular imaging surveillance both in the presurgical setting to monitor aortic aneurysm and other complications, but also in the post-surgical setting to monitor for surgical complications and continued growth or dissection of the residual native aorta. Currently, the primary metric used to estimate the risk of dissection and inform candidacy for surgical management is maximal aortic diameter [5, 6]. Unfortunately, this metric is a poor predictor of dissection development, with a recent study estimating that ∼80% of dissection patients (both type A and type B) have a maximal aortic diameter below standard surgical thresholds (5.5 cm) at the time of dissection [7, 8]. In a study of Marfan patients who developed type B dissection during the imaging surveillance, the average pre-dissection diameter of the affected segment was normal at 28 mm, highlighting a critical need for better risk assessment techniques in this population [9].

Aortic growth is a complex phenomenon driven by a wide range of biomechanical processes such as inflammation, intrinsic structural defects related to CTD, wall constituent turnover and hypertension [10]. While the exact sequence of events leading to the initiation of aortic dissection remains poorly understood, pathological, computational and animal studies have demonstrated common pathways of medial degeneration, including mucoid extracellular matrix accumulation, elastic fibre fragmentation and smooth muscle cell necrosis, that result in progressive loss of aortic wall integrity and ultimately the intimal tearing and wall delamination [11]. Recent reports have highlighted that the local transmural wall stress during a cardiac cycle can influence long-term growth and remodelling of the aortic wall through stress-mediated changes in aortic wall tissue composition [12–14]. In addition, a prior study investigating the biomechanical effects of pooling of proteoglycans within the aortic wall—a common abnormality in CTD—demonstrated that such accumulations and the resultant osmotic swelling can lead to localized concentrations of wall stress that are sufficient to disrupt the extracellular matrix and initiate tearing [15].

Regardless of the exact mechanism of aortic dissection initiation, the progressive loss of aortic wall integrity caused by medial degeneration also results in aortic growth, a concept that has been termed as mechanobiological instability [16]. However, aortic growth is often slow and small in magnitude and, thus, undetected by current diameter-based measurement approaches due to the high degree of measurement variability (on the order of ±1–5 mm) [17]. Vascular deformation mapping (VDM) is a recently developed image analysis technique that may overcome these limitations [18]. VDM measures 3-dimensional (3D) aortic wall deformation between 2 computed tomography angiography (CTA) scans. This 3D deformation allows for accurate characterization of the localized patterns of aortic wall enlargement that could help detect early adverse aortic remodelling leading to acute adverse events.

In this study, we investigate the hypothesis that areas of focal aortic enlargement, via their association with wall instability, will co-localize spatially with the site of an intimal tear in patients with thoracic aortic disease and CTD who developed aortic dissection during the course of clinical imaging surveillance. Furthermore, we investigate the relationship between the location of intimal tear formation, computationally obtained spatial distribution of cyclic aortic wall stress, and the pattern of long-term aortic wall enlargement obtained via VDM analysis.

METHODS

Patient identification and characteristics

Subjects were identified retrospectively from an internal database of patients referred to the Department of Cardiac Surgery and Department of Interventional Radiology at our institution with available pre-dissection CTA imaging between January 2011 and January 2019. These patients were recruited to an Institutional Review Board approved study (Protocol # HUM00133798), on 18 August 2017 with waiver of informed consent. During this period, we identified a total of 31 patients with pre-dissection CTA scans,

although 12 were excluded for having only 1 pre-dissection CTA (the VDM growth analysis requires 2 studies), 8 patients were excluded due to non-ECG-gated CTA scans, 5 patients were excluded for surgical repair of an adjacent segment in the pre-dissection intervals, and finally, 2 patients were excluded for poor quality CT images (e.g. poor contrast opacification, motion artefact). Of the remaining 4 patients, 3 had confirmed diagnosis of CTD and, thus in order to maximize the homogeneity of the population, the single non-CTD patient was excluded.

Computed tomography angiography imaging

All CTA studies were performed at our institution on a 64-slice scanner (GE Healthcare, Milwaukee, WI, USA) after intravenous injection of 120 ml iopamidol contrast (Isoview 370, Bracco Diagnostics, Milan, Italy). ECG-gating was used in all CTA studies. CTA data were reconstructed at 75% of the R-R interval with 1.25-mm slice thickness and 0.625-mm slice interval.

Vascular deformation mapping

Methods for VDM have been described in detail in previous work [12]. However, in brief, the VDM technique involves the following steps:

i. Segmentation: the thoracic aorta, from the aortic valve to 10 mm beyond the coeliac artery, is first segmented using a threshold-based approach followed by manual adjustments and the surface structure is based on this segmentation. Aortic segmentation and automated centreline calculation are performed using Mimics 21.0 (Materialise NV, Leuven, Belgium) and the segmentation is also used to generate a mask that is used to constrain the registration step.
ii. Image registration: deformable image registration was performed between serial CTA studies using a custom MATLAB interface to the Elastix open-source software (Utrecht, Netherlands). Registration was performed in 2 steps, first with an affine registration to approximately align the 2 segmentations, followed by non-rigid, multi-resolution B-spline registration using mutual information as the similarity metric.
iii. Deformation quantification: deformation between pre-dissection CTA studies was quantified as the determinant of the 3D spatial Jacobian calculated from the final optimized image transform and normalized by the time interval ($|J|$/year) to obtain a deformation rate. The Jacobian determinant represents volumetric change, and thus, a growth of 0.2 J/year at a point on the aortic wall surface can be interpreted as a 20% volumetric change over the time interval at that point. Deformation rate values (J/year) were linearly interpolated to the vertex points of the baseline aortic segmentation surface for display. Positive values of J represent aortic wall expansion (yellow-red colour scale), aortic wall compression by J values <0 (blue) and unchanged aortic wall geometry by $J \approx 0$ (green). For further information on the VDM methods, please refer to the Supplementary Material.

Computational stress analysis

An aortic model was constructed from the baseline mid-diastolic phased CTA image data using the in-house computational haemodynamics modelling environment, CRIMSON (CardiovasculaR Integrated Modelling and SimulatiON, www.crimson.software) [19]. The vessel wall geometry was obtained by creating 2-dimensional segmentation contours along the vessel centreline, followed by subsequent lofting to create a geometric coronary artery disease model. The aortic wall was modelled as a thin shell using a finite element formulation. To account for the non-linear behaviour of the vessel wall, the aortic wall is characterized by a Neo-Hookean material model. The Neo-Hookean model material stiffness constant (c) and wall thickness (t) were varied from $c = 1$ MPa, $t = 2$ mm for the ascending aorta to $c = 2$ MPa, $t = 1.6$ mm for the descending aorta [15, 20]. For the Dacron graft, uniform coefficients were assigned to the entire surface: $c = 50$ MPa and $t = 0.5$ mm [15, 20]. For each subject, the aortic model was first prestressed to the patient-specific diastolic pressure (listed in Table 1) using a forwards incremental prestress strategy [21]. This procedure identifies the *in vivo* diastolic state of stress in the aortic wall. Subsequently, the aortic wall is loaded from diastolic pressure to systolic pressure to identify the distribution of cyclic transmural wall stresses. A simplified conceptual workflow of both the VDM and the computational analysis approaches of this work is shown in Fig. 1. A more in-depth description of the computational methods can be found in the Supplementary Material.

RESULTS

Three patients are described in this series and will be discussed below in a case-by-case manner. A summary of the patient demographics and the timeline is provided in Table 1. Antihypertensive medication, dose and frequency for each patient were constant over the entire course of surveillance imaging leading up to the dissection. Table 2 summarizes the 3D growth, transmural wall stress and CTA follow-up for each patient.

Patient 1

The first patient was a 30-year-old female with Marfan syndrome and scoliosis, a prior history of Bentall repair at age 15 and multiple prior mitral valve procedures. She was an active smoker at baseline CT scan but had no other risk factors for cardiovascular disease. The interval between her 2 surveillance CT scans was 2.3 years and her thoraco-abdominal aorta was reported to have enlarged from 3.6 to 4.2 cm in maximal diameter over that period by clinical radiological assessment. The recorded pulse pressure at the baseline CT scan and the follow-up CT scan increased from 36 to 52 mmHg. By VDM analysis, peak growth was found in the supraceliac aorta region (0.29 J/year) and co-localized with the site of subsequent intimal tear formation. The peak stress value (0.35 MPa) was observed in this same region, ~1 cm proximal to the origin of the coeliac trunk (Fig. 2). The time interval between the second CT scan and the date of dissection was 12 months.

Patient 2

The second patient was a 52-year-old male with Marfan syndrome, hypertension, dyslipidaemia and history of ascending aortic aneurysm, who underwent valve-sparing repair 20 months prior to baseline surveillance scan. His blood pressure had been well-controlled with oral metoprolol 25 mg twice daily and

Table 1: Patient characteristics including antihypertensive medication and the last reported blood pressure medication before the onset of dissection

Patient	Age	Gender	Comorbidities	Prior surgery	Antihypertensive medication	BP at baseline CTA (mmHg)	BP at follow-up CTA (mmHg)
1	30	Female	Marfan syndrome	Bentall procedure, mitral valve repair	Furosemide 25 mg daily, atenolol 25 mg daily	109/73	124/72
2	52	Male	Marfan syndrome, hypertension, dyslipidaemia	David procedure	Furosemide 2 0 mg daily, metoprolol 50 mg daily	104/65	120/80
3	40	Male	Loeys-Dietz syndrome, hypertension, dyslipidaemia	AVR with ascending tube repair, redo ascending repair with TAR	Metoprolol 100 mg daily	114/65	145/80

AVR: aortic valve replacement; BP: blood pressure; CTA: computed tomography angiography; TAR: total arch replacement.

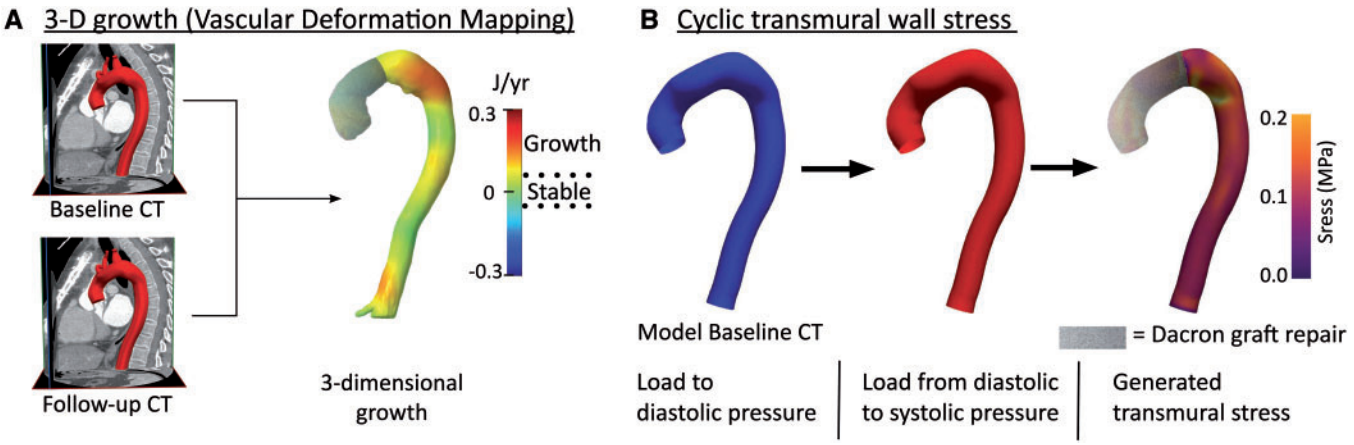

Figure 1: Overview of methodology of (**A**) 3D growth analysis through a vascular deformation map and (**B**) computational analysis of transmural wall stress. CT: computed tomography; 3D: 3-dimensional.

Table 2: Summary of 3D growth and transmural wall stress outcomes for each patient

	Case 1	Case 2	Case 3
Follow-up baseline to second CTA (years)	2.3	2.1	2.1
2-D diameter change (mm/year)	1.8	1.0	1.5
Peak growth (J/year)	0.29	0.14	0.25
Peak stress (MPa)	0.35	0.14	0.14
Follow-up second CTA to dissection (months)	11.7	3.5	11.8

CTA: computed tomography angiography; 2-D: 2-dimensional; 3D: 3-dimensional.

furosemide 20 mg daily. Pulse pressure was 39 mmHg at baseline CT scan and 40 mmHg at the follow-up CT scan. The interval between his 2 surveillance CT scans was 2.1 years. Radiology reports did not describe any significant changes between the 2 surveillance CTA studies. A focal area of growth (0.14 J/year) was identified by VDM along the posterior wall of the distal arch in close proximity of the location of the subsequent intimal tear. The site of peak transmural wall stress (0.14 MPa) was located along the posterior distal arch at the lesser curvature, in close proximity and just proximal to the site of the intimal tear (Fig. 3). The time interval between the follow-up scan and the date of dissection was 3.5 months.

Patient 3

The third patient was a 40-year-old male with Loeys–Dietz syndrome, hypertension, dyslipidaemia and a history of DeBakey type II aortic dissection, which had been previously repaired at an outside hospital. However, a redo repair was performed at our institution due to residual dissection and proximal growth, using a modified root repair due to frail sinus and coronary tissue, with concurrent ascending aortic and total arch repairs, including the innominate and left carotid artery. During the postoperative period, blood pressure remained well controlled over a 2.1-year interval between surveillance CT scans using oral metoprolol 100 mg daily with a pulse pressure of 49 mmHg at the baseline scan and 65 mmHg at the follow-up scan. Peak growth was 0.25 J/year and was measured at the distal aortic arch. Peak transmural wall stress was 0.14 MPa, located at the distal aortic arch. The sites of peak growth and peak transmural stress co-localized with the region of the subsequent intimal tear (Fig. 4).

DISCUSSION

Despite the poor performance of aortic diameter in predicting the risk of dissection, with 50–60% of patients dissecting at a normal or mildly dilated aortic diameter (<45 mm) [7, 8], it remains the most commonly used metric in clinical practice. Key

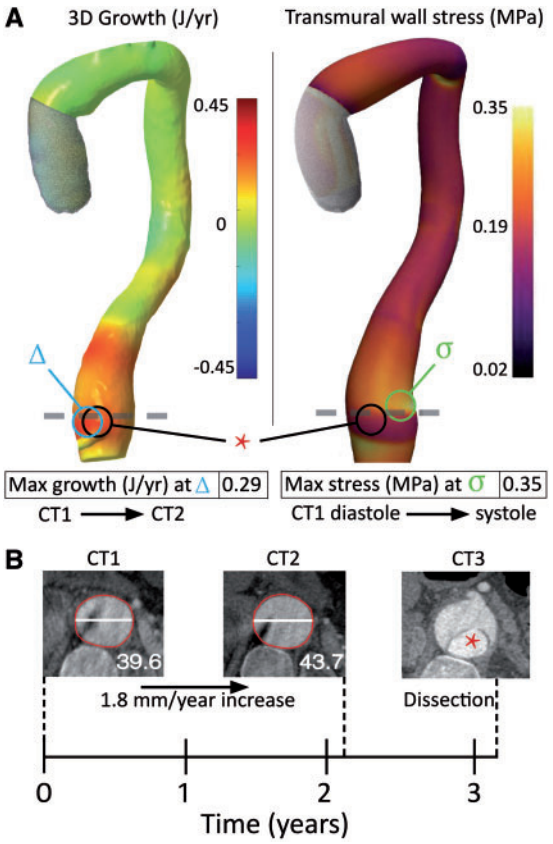

Figure 2: 3D growth (**A**, left) and computational cyclic transmural stress (**A**, right) results for patient 1. The site of intimal tear (star) co-localized with the region of peak growth (delta) and the region of peak transmural stress (sigma) in the supraceliac aorta. Serial CT images at the level of subsequent tear are shown below (**B**). The greyed area reflects graft material from aortic repair. Of note, intraluminal artefact from metallic spinal hardware is seen on CT1 and CT2 images. CT: computed tomography; 3D: 3-dimensional.

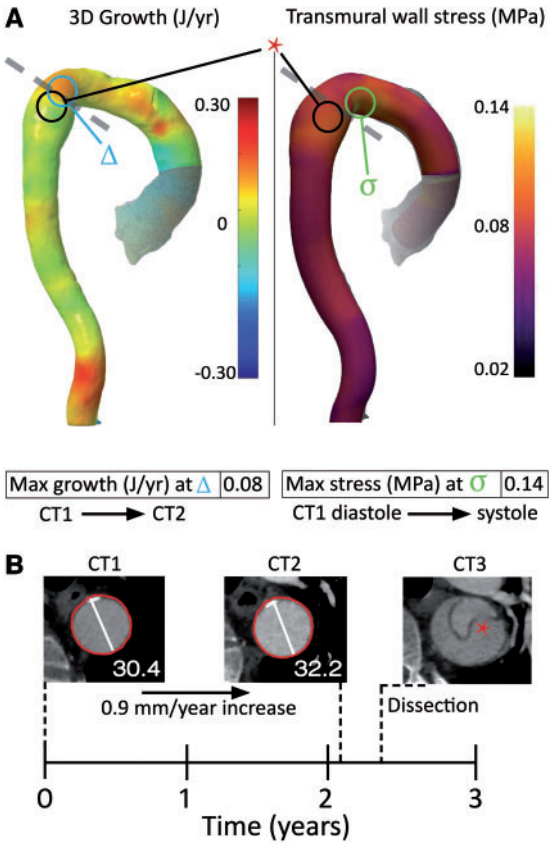

Figure 3: 3D growth (**A**, left) and computational cyclic transmural stress (**A**, right) results for patient 2. The site of intimal tear (star) co-localized with a region of peak growth (delta) and the region of peak transmural stress (sigma) in the distal arch. Serial CT images at the level of subsequent tear are shown below (**B**). The greyed area reflects graft material from aortic repair. CT: computed tomography; 3D: 3-dimensional.

limitations of a diameter-based approach are that this method represents aortic growth as a circumferentially uniform process, measures growth primarily at the site of maximal aortic diameter and is characterized by a high degree of measurement variability. Furthermore, diameter measurements overlook the 3D features of aortic growth. A final potential reason for the obvious disconnect between diameter and dissection risk may be that 3D growth is a dynamic measure, unlike maximal diameter, and maybe more reflective of the underlying pathological factors that eventually lead to long-term growth and progressive loss of wall integrity. It seems logical that an actively growing 4-cm diameter aorta has less structural integrity than a stable 6-cm aorta.

Beyond morphological changes such as aortic growth, there have been recent reports indicating the role of transmural wall stress driving long-term growth and remodelling of aortic tissue [22, 23]. For instance, in the context of hypertension, increased blood pressure leads to locally elevated circumferential wall stress, which promotes matrix synthesis, often via local production of angiotensin-II, and exacerbates arterial wall stiffening. This stiffening further causes an increase in the pulse wave velocity that can lead to augmented central blood pressure, thereby initiating an insidious positive feedback loop that results in progressive worsening [14]. In addition, prior computational research has suggested that the accumulation of pools of proteoglycans within the wall and subsequent osmotic swelling can lead to localized concentrations of wall stress that may initiate intimal tearing [15] and recent evidence has confirmed such accumulations through clinical-pathological samples of CTD patients with aortic dissection [24]. Despite these reports, the contribution of cyclical transmural wall stress in driving long-term adverse aortic events such as aortic dissection has not been explored in detail.

To address these issues, we combine a 3D assessment of aortic growth using an advanced image analysis technique, VDM and a computational analysis of cyclic transmural wall stress. We submit that the VDM may be better suited to investigate the link between aortic dimensions and the risk of aortic dissection given that it is less prone to measurement variability and capable of depicting the 3D nature of growth. Furthermore, a computational analysis of cyclic transmural stress in baseline CTA geometry could indicate the areas of aortic wall that are most vulnerable to aortic dissection due to the reported stress-mediated turnover of aortic constituents reported in earlier growth and remodelling reports [12–14]. This 2-pronged approach can allow for a sophisticated morphological and biomechanical assessment that may improve our current understanding of the pathogenesis of aortic dissection.

Our results revealed that the site of intimal tear co-localized with both focal areas of aortic growth and with cyclic transmural wall stress, supporting our hypothesis that the risk of dissection

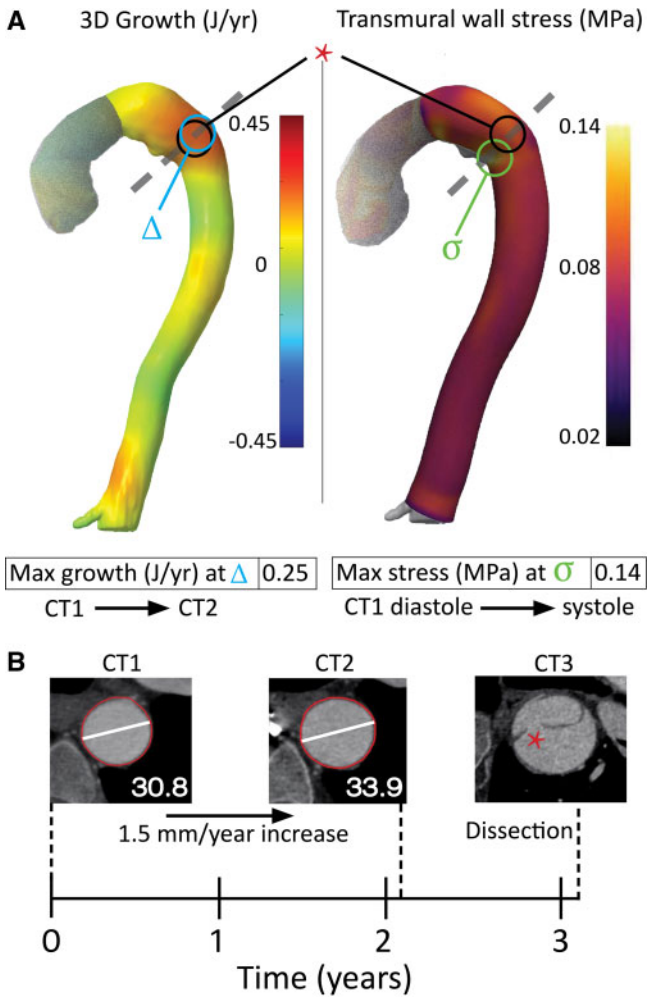

Figure 4: 3D growth (**A**, left) and computational cyclic transmural stress (**A**, right) results for patient 3. The site of intimal tear (star) co-localized with a region of peak growth (delta) and the region of peak transmural stress (sigma) in the distal arch. Serial CT images at the level of subsequent tear are shown below (**B**). The greyed area reflects graft material from aortic repair. CT: computed tomography; 3D: 3-dimensional.

may be highest at locations where insufficient wall integrity (e.g. growth) and abnormal wall stress intersect. Our study consisted of 3 patients who all suffered from CTD. Due to an imbalance in the signalling pathway of transforming growth factor-beta and associated downstream cellular and extracellular structural alterations, patients with CTD are known to exhibit an accelerated growth profile compared to patients without CTD [25]. It has been suggested that prior aortic repair is an increased risk factor for TBAD in patients with Marfan syndrome, as was observed in all 3 patients in our study. The preliminary findings in this study would be more optimally validated if the outcomes of our current series where to be compared to both CTD patients with dissection but without any prior aortic repair, however, serial CTA studies in this population were not available for analysis at our centre.

To our knowledge, the results of this study are the first to demonstrate a spatial correlation between the site of intimal tear dissection, peak cyclic transmural wall stress and peak focal growth using clinical imaging data from TBAD patients. Our results, while admittedly still preliminary, suggest a potential new approach to determine the risk of dissection in CTD patients undergoing imaging surveillance for thoracic aortic disease. Non-invasive assessment of focal growth (rather than the maximal diameter) and cyclical transmural wall stress may more closely represent pathological changes in the aortic wall that are currently thought to play a role in the initiation of aortic dissection but which are difficult to assess using currently available methods. Considering that both the VDM and the computational technique utilize routine ECG-gated CTA data—the mainstay of aortic disease surveillance—if future research confirms the predictive value of the proposed computational indices presented here, these findings would be poised for translation into clinical practice.

Limitations

There are several limitations to this study, which include the following:

i. The number of patients in this study was small, as we were limited to patients with 2 available pre-dissection ECG-gated CTAs to perform VDM analysis, which is an uncommon occurrence. In addition, all 3 patients had CTD, so while this may only represent a small fraction of patients with TBAD, these patients are at higher risk of dissection and are more likely to receive regular imaging surveillance, so our findings may be best applied to this population.
ii. There was a variable amount of time between the last surveillance CT and dissection event (between about 4–12 months), however, we were limited by available CT data, and while the exact changes in aortic wall geometry closer to the date of dissection are unknown, it is reassuring that areas of aortic growth co-localized with the site of intimal tear in all cases.
iii. We were not able to assess the potential co-localization of abnormal hemodynamics (e.g. elevated wall shear stress) with the site of intimal tear, mostly owing to a lack of patient-specific hemodynamic data (echo or phase-contrast magnetic resonance imaging). However, the contribution of abnormal wall shear stress in the dissection of the ascending aorta (type A) related to post-stenotic jets and less so in the dissection of the descending thoracic aorta (type B) as in all of the patients in our study [26].
iv. This work utilized a non-linear thin shell description for the aortic wall via a Neo-Hookean material model using available literature data for tissue properties. Alternative multi-layer material models and the use of patient-specific material parameters can further improve the computational predictions of aortic wall stress. Future studies will aim to obtain blood pressures, next to multiphase ECG-gated CTA data, in order to derive the patient-specific structural stiffness through distensibility assessment.

CONCLUSION

In conclusion, this multiparametric analysis co-localization of pre-dissection focal aortic growth and cyclic transmural stress with the site of an intimal tear in TBAD patients. Our results support the roles of stress concentrations and loss of aortic wall structural integrity that have been suggested to contribute to dissection initiation. While future work is needed to validate our findings in a larger population and compare to a cohort of patients who did not develop dissection events during imaging surveillance, we believe the results of this study support our

hypothesis on the mechanisms driving aortic growth and should motivate further investigation into the prognostic significance of transmural wall stress and VDM growth mapping, and most importantly their intersection. Given the recent availability of such advanced aortic wall analysis techniques, we may finally be approaching a point where dissection risk-stratification can move from a poorly predictive diameter-based approach to a sophisticated morphological and biomechanical assessment that better aligns with our current understanding of the pathogenesis of aortic dissection initiation.

SUPPLEMENTARY MATERIAL

Supplementary material is available at *EJCTS* online.

Funding

This work was supported by Joe D. Morris Professorship, David Hamilton Fund and the Phil Jenkins Breakthrough Fund to H.J.P; European Research Council under the European Union's Seventh Framework Programme (FP/2007–2013) [ERC Grant Agreement No. 307532], National Institutes of Health [R01 HL105297, U01 HL135842], the Edward B. Diethrich Professorship, the Bob and Ann Aikens Aortic Grants Program and the Frankel Cardiovascular Center and National Science Foundation [grant 1531752] to C.A.F.; and Radiologic Society of North America Research Scholar Grant [RSCH 1801] and National Institutes of Health [R44 HL145953] to N.S.B.

Conflict of interest: Nicholas S. Burris entitled to royalties related to licensure of intellectual property for Vascular Deformation Mapping technique. All other authors declared no conflict of interest.

Author contributions

Ignas B. Houben: Conceptualization; Data curation; Formal analysis; Investigation; Methodology; Resources; Validation; Visualization; Writing—original draft). **Nitesh Nama:** Conceptualization; Data curation; Formal analysis; Investigation; Methodology; Project administration; Resources; Software; Validation; Writing—original draft. **Frans L. Moll:** Supervision; Writing—review & editing. **Joost A. van Herwaarden:** Supervision; Writing—review & editing. **David A. Nordsletten:** Conceptualization; Supervision; Writing—review & editing. **David M. Williams:** Conceptualization; Supervision; Writing—review & editing. **Himanshu J. Patel:** Conceptualization; Funding acquisition; Methodology; Resources; Supervision; Writing—review & editing. **C. Alberto Figueroa:** Conceptualization; Funding acquisition; Methodology; Resources; Software; Supervision; Writing—review & editing. **Nicholas S. Burris:** Conceptualization; Data curation; Formal analysis; Funding acquisition; Investigation; Methodology; Project administration; Resources; Software; Supervision; Validation; Visualization; Writing—original draft; Writing—review & editing.

REFERENCES

[1] Hiratzka LF, Bakris GL, Beckman JA, Bersin RM, Carr VF, Casey DE *et al.* 2010 ACCF/AHA/AATS/ACR/ASA/SCA/SCAI/SIR/STS/SVM guidelines for the diagnosis and management of patients with thoracic aortic disease. Anesth Analg 2010;111:279–315.

[2] Riambau V, Böckler D, Brunkwall J, Cao P, Chiesa R, Coppi G *et al.* Management of descending thoracic aorta diseases: clinical practice guidelines of the European Society for Vascular Surgery (ESVS). Eur J Vasc Endovasc Surg 2017;53:4–52.

[3] Collins JS, Evangelista A, Nienaber CA, Bossone E, Fang J, Cooper JV *et al.* Differences in clinical presentation, management, and outcomes of acute type A aortic dissection in patients with and without previous cardiac surgery. Circulation 2004;110(Suppl 1):II237–42.

[4] Vilacosta I, Aragoncillo P, Cañadas V, San Román JA, Ferreirós J, Rodríguez E. Acute aortic syndrome: a new look at an old conundrum. Heart 2009;95:1130–9.

[5] Elefteriades JA, Farkas EA. Thoracic aortic aneurysm. clinically pertinent controversies and uncertainties. J Am Coll Cardiol 2010;55:841–57.

[6] Kim JB, Spotnitz M, Lindsay ME, MacGillivray TE, Isselbacher EM, Sundt TM. Risk of aortic dissection in the moderately dilated ascending aorta. J Am Coll Cardiol 2016;68:1209–19.

[7] Trimarchi S, Jonker FHW, Froehlich JB, Upchurch GR, Moll FL, Muhs BE *et al.* Acute type B aortic dissection in the absence of aortic dilatation. J Vasc Surg 2012;56:311–16.

[8] Berezowski M, Kosiorowska K, Beyersdorf F, Riesterer T, Jasinski M, Plonek T *et al.* Modelling of predissection aortic size in acute descending aortic dissection. Interact CardioVasc Thorac Surg 2019;29:124–9.

[9] Den Hartog AW, Franken R, Zwinderman AH, Timmermans J, Scholte AJ, van den Berg MP *et al.* The risk for type B aortic dissection in Marfan syndrome. J Am Coll Cardiol 2015;65:246–54.

[10] Goldfinger JZ, Halperin JL, Marin ML, Stewart AS, Eagle KA, Fuster V. Thoracic aortic aneurysm and dissection. J Am Coll Cardiol 2014;64:1725–39.

[11] Halushka MK, Angelini A, Bartoloni G, Basso C, Batoroeva L, Bruneval P *et al.* Consensus statement on surgical pathology of the aorta from the Society for Cardiovascular Pathology and the Association For European Cardiovascular Pathology: II. Noninflammatory degenerative diseases—nomenclature and diagnostic criteria. Cardiovasc Pathol 2016;25:247–57.

[12] Valentin A, Humphrey JD, Holzapfel GA. A finite element-based constrained mixture implementation for arterial growth, remodeling, and adaptation: theory and numerical verification. Int J Numer Method Biomed Engng 2013;29:822–49.

[13] Bersi MR, Bellini C, Wu J, Montaniel KRC, Harrison DG, Humphrey JD. Excessive adventitial remodeling leads to early aortic maladaptation in angiotensin-induced hypertension. Hypertension 2016;67:890–6.

[14] Humphrey JD, Harrison DG, Figueroa CA, Lacolley P, Laurent S. Central Artery stiffness in hypertension and ageing a problem with cause and consequence. Circ Res 2016;118:379–81.

[15] Roccabianca S, Bellini C, Humphrey JD. Computational modelling suggests good, bad and ugly roles of glycosaminoglycans in arterial wall mechanics and mechanobiology. J R Soc Interface 2014;11:20140397.

[16] Cyron CJ, Wilson JS, Humphrey JD. Mechanobiological stability: a new paradigm to understand the enlargement of aneurysms? J R Soc Interface 2014;11:20140680.

[17] Asch FM, Yuriditsky E, Prakash SK, Roman MJ, Weinsaft JW, Weissman G *et al.* The need for standardized methods for measuring the aorta multimodality core lab experience from the GenTAC registry. JACC Cardiovasc Imaging 2016;9:219–26.

[18] Burris NS, Hoff BA, Kazerooni EA, Ross BD. Vascular deformation mapping (VDM) of thoracic aortic enlargement in aneurysmal disease and dissection. Tomography 2017;3:163–73.

[19] Arthurs CJ, Figueroa CA. CRIMSON Software, Documentation and Downloads. 2019. http://www.crimson.software/downloads.html (10 January 2019, date last accessed).

[20] Tremblay D, Zigras T, Cartier R, Leduc L, Butany J, Mongrain R *et al.* A comparison of mechanical properties of materials used in aortic arch reconstruction. Ann Thorac Surg 2009;88:1484–91.

[21] Grytz R, Downs JC. A forward incremental prestressing method with application to inverse parameter estimations and eye-specific simulations of posterior scleral shells. Comput Methods Biomech Biomed Engin 2013;16:768–80.

[22] Taber LA, Humphrey JD. Stress-modulated growth, residual stress, and vascular heterogeneity. J Biomech Eng 2001;123:528–35.

[23] Holzapfel GA, Gasser TC, Ogden RW. A new constitutive framework for arterial wall mechanics and a comparative study of material models. J Elast 2000;61:1–48.

[24] Cikach FS, Koch CD, Mead TJ, Galatioto J, Willard BB, Emerton KB *et al.* Massive aggrecan and versican accumulation in thoracic aortic aneurysm and dissection. JCI Insight 2018;3:pii: 97167.

[25] Humphrey JD. Possible mechanical roles of glycosaminoglycans in thoracic aortic dissection and associations with dysregulated transforming growth factor-β. J Vasc Res 2013;50:1–10.

[26] van Ooij P, Markl M, Collins JD, Carr JC, Rigsby C, Bonow RO *et al.* Aortic valve stenosis alters expression of regional aortic wall shear stress: new insights from a 4-dimensional flow magnetic resonance imaging study of 571 subjects. J Am Heart Assoc 2017;6:1–13.